Motional Properties of Two Vicinally Disubstituted Trisaccharides As Studied by Multiple-Field Carbon-13 NMR Relaxation

Alexandra Kjellberg,[†] Torgny Rundlöf,[†] Jozef Kowalewski,[‡] and Göran Widmalm*[,†]

Department of Organic Chemistry and Division of Physical Chemistry, Arrhenius Laboratory, Stockholm University, S-106 91 Stockholm, Sweden

Received: May 7, 1997; In Final Form: November 3, 1997

Multiple-field carbon-13 NMR relaxation measurements have been performed on the two vicinally disubstituted trisaccharides β-D-Glc*p*-(1 → 2)[β-D-Glc*p*-(1→3)]-α-D-Glc*p*-OMe (**1**) and β-D-Glc*p*-(1 → 2)[β-D-Glc*p*-(1 → 3)]-α-D-Man*p*-OMe (**2**). Trisaccharide **1** has trans disubstitution of the terminal β-glucosyl residues, while trisaccharide **2** has cis disubstitution. Carbon-13 T_1 and T_2 relaxation and NOE measurements were performed outside the extreme-narrowing regime at three temperatures 283, 303, and 323 K and four magnetic field strengths 6.3, 9.4, 11.7, and 14.1 T. The obtained relaxation rates and NOE factors, averaged for each sugar residue, were fitted to overall and internal correlation times and order parameters using the Lipari−Szabo "model-free" formalism. The 2,3-disubstituted *O*-methyl glycoside showed fairly high-order parameters, $S^2 \approx 0.9$, for both trisaccharides at all three temperatures, while the terminal glucosyl residues of **1** and **2** showed lower and slightly temperature-dependent order parameters, $S^2 \approx 0.8$. In **1**, the terminal residues were found to have similar motional properties and an internal correlation time of ∼60 ps could be obtained from a simultaneous three-parameter fit at 303 K. Similar results were obtained for trisaccharide **2**. This study shows that the branch-point residue displays more restricted mobility than the terminal residues in both trisaccharides and that internal motions can be detected for small oligosaccharides using NMR relaxation measurements and the Lipari−Szabo model-free formalism.

Introduction

The three-dimensional structure of biomolecules in solution may be described by a model based on atomic coordinates. It is an advantage if this description can be extended by including the dynamic information, such as the degree of flexibility of certain regions in the molecule. Based on this, the question of the applicability of the static, often structurally averaged, molecular picture can also be addressed.

A way to investigate the dynamics of molecules is by measurement of nuclear-spin relaxation rates, which for isotopically enriched proteins include carbon-13 and nitrogen-15, both of spin $^1/_2$. The heteronuclear relaxation parameters T_1 and T_2 and NOE can be measured as a function of magnetic-field strength, and the dynamical information from the nuclear-spin relaxation measurements is accessible through the spectral-density functions, which determine the relaxation rates.[1] Unless special schemes are chosen,[2] the interpretation of relaxation data requires a model. The Lipari−Szabo "model-free" approach[3] has found numerous applications to proteins[4−6] and nucleic acids.[7,8] In the Lipari−Szabo approach, the spectral-density functions depend on a few parameters: a generalized order parameter (which is a measure of the spatial restriction of the internal motion), the global overall correlation time, and an effective local correlation time for internal motions.

The conformation(s), flexibility, and dynamics of carbohydrates are of great interest not least because of the important role carbohydrates play in many biological processes, e.g., protein folding and protein sorting in biosynthetic traffic.[9] The processes involving molecular recognition are especially noteworthy,[10] including, for example, parasitic, viral, and bacterial infection, fertilization, cancer, or inflammatory processes. Investigations of conformational flexibility and the dynamics of carbohydrates employ to a large extent NMR spectroscopy and molecular-modeling techniques.[11]

In the latter, a molecular model based on a molecular-mechanics force field is commonly used. For the study of the conformational space, a systematic grid search employing nonrestrained or restrained energy minimization may be used for locating low-energy regions or for generating a Ramachandran map, respectively. In these procedures the major degrees of freedom for an oligosaccharide are subject to variation. These are the angles ϕ and ψ of the glycosidic linkage and, for 6-substituted sugar residues, also the dihedral angle ω. Monte Carlo (MC) simulations are suitable for conformational problems, especially of larger oligosaccharides, in which the increased number of degrees of freedom make a nonsystematic search more tractable.[12] From MC simulations, averaged properties may also be calculated for comparison with experimental data.

When information on the evolution with time is desired, molecular-dynamics (MD) simulations can be performed.[13] The molecule is either simulated in vacuo or solvated, commonly in water, and the simulation time is usually on the order of hundreds of picoseconds to a few nanoseconds. The simulations can give insight into molecular structures and processes for which only averaged information is available from experimental data. Calculations of, for example, spectral-density functions,[14,15] order parameters,[16] and relaxation times[17] can be made from these MD simulations. In the above techniques, the flexibility and dynamics obtained for carbohydrates are depend-

* Corresponding author (fax +46 8 154908).
[†] Department of Organic Chemistry.
[‡] Division of Physical Chemistry.

S1089-5647(97)01542-3 CCC: $15.00
Published on Web 01/22/1998

ent on the force field employed. Experimental investigations on the dynamics and flexibility thus provide additional information for the assessment of various force fields used in molecular modeling, besides the results from the study per se.

NMR studies on carbohydrates in solution give information on structure, conformation, flexibility, and dynamics in general.[18,19] The techniques most often used are homonuclear ^{1}H, ^{1}H nuclear Overhauser effects (NOEs) in the form of 1D- or 2D-NOESY experiments, measurements of heteronuclear long-range coupling constants over the glycosidic linkage,[20,21] and the measurement of ^{13}C spin−lattice and spin−spin relaxation times in conjunction with ^{13}C, ^{1}H heteronuclear NOEs.[22] The experimental data can then be compared with molecular models obtained from simulations, such as MC or MD simulations. We have previously made use of the Lipari−Szabo "model-free" approach for the interpretation of relaxation data obtained from oligosaccharides.[23−27] In these studies different degrees of flexibility and dynamics have been found, depending on molecular structure, i.e., substitution pattern or anomeric configuration.

In contrast to other biomolecules, such as proteins and nucleic acids, a high degree of branching may be observed for carbohydrates. Positional isomers as well as the degree of branching lead to a large diversity in carbohydrate structures, e.g., those from glycoproteins or polysaccharides. The sites of substitution, as well as the anomeric (i.e., α- or *β*-) and the absolute (i.e., D- or L-) configurations of the sugar residues at the branch-point residue, determine the three-dimensional structure and the dynamic behavior of the sugar residues in the region where branching occurs.

This study addresses the motional properties of two vicinally disubstituted trisaccharides in which trans substitution occurs for the trisaccharide *β*-D-Glc*p*(1 → 2)[*β*-D-Glc*p*(1 → 3)]-α-D-Glc*p*-OMe (**1**) and cis substitution occurs for the trisaccharide *β*-D-Glc*p*(1 → 2)[*β*-D-Glc*p*(1 → 3)]-α-D-Man*p*-OMe (**2**). Heteronuclear relaxation parameters T_1 and T_2 and NOE have been measured at four magnetic field strengths and at three temperatures. The data have subsequently been analyzed using the Lipari−Szabo "model-free" approach.

Theory

The relaxation of proton-bearing carbon-13 nuclei is usually dominated by the dipole−dipole (DD) interaction with neighboring protons. Sometimes one also has to consider the chemical shift anisotropy (CSA) and/or the cross-correlation of DD and CSA interactions as sources of relaxation.[28] Measurements of carbon-13 longitudinal relaxation are usually performed under the conditions of broad-band proton decoupling, which results in single-exponential processes characterized by the rate T_1^{-1} and vanishing DD−CSA cross-correlation effects.[29] For measurements of transverse relaxation, one usually does not use decoupling during the relaxation period, and other schemes for elimination of the cross-correlation effects therefore must be employed.[30,31] A simple exponential relaxation, characterized by the rate T_2^{-1}, is then obtained also in this case. The ^{13}C, ^{1}H NOE factor $(1 + \eta)$ is a measure of the intensity increase of the carbon signal as a result of cross-relaxation between a carbon and proton(s) under ^{1}H-decoupling conditions.

The relaxation parameters can be expressed in terms of spectral-density functions taken at different combinations of the carbon (ω_C) and proton (ω_H) Larmor frequencies. For carbons relaxed by the dipole−dipole relaxation mechanism caused by a single directly bonded proton, the relaxation parameters T_1^{-1}, T_2^{-1}, and η are related to the spectral densities by the following equations:[1,3]

$$T_1^{-1} = \frac{1}{4}(\mathrm{DCC})^2[J(\omega_H - \omega_C) + 3J(\omega_C) + 6J(\omega_H + \omega_C)] \quad (1)$$

$$T_2^{-1} = \frac{1}{8}(\mathrm{DCC})^2[4J(0) + J(\omega_H - \omega_C) + 3J(\omega_C) + 6J(\omega_H) + 6J(\omega_H + \omega_C)] \quad (2)$$

$$\eta = \left(\frac{\gamma_H}{\gamma_C}\right)\frac{6J(\omega_H + \omega_C) - J(\omega_H - \omega_C)}{J(\omega_H - \omega_C) + 3J(\omega_C) + 6J(\omega_H + \omega_C)} \quad (3)$$

The dipolar coupling constant $\mathrm{DCC} = [\mu_0/(4\pi)]\gamma_C\gamma_H\hbar r_{CH}^{-3}$ is related to the strength of the dipolar interaction between the two spins, and consequently, DCC is dependent on the distance (r_{CH}) between these spins. A value of 109.8 pm is used for r_{CH}, corresponding to a dipolar coupling constant of 143.40 kHz. For carbons with two protons directly attached, such as the exocyclic CH_2 carbons in sugars, the expressions for T_1^{-1} and T_2^{-1} should be multiplied by 2 while the expression for η remains the same, provided that there is no cross-correlation between motions of individual CH vectors.

To interpret the relaxation parameters in terms of reorientational dynamics, the "model-free" approach by Lipari and Szabo[3] is often used. In this model two kinds of motions are assumed to modulate the interaction causing relaxation: a rapid, local motion and a slower, global motion. If the two motions are statistically independent and if the global molecular reorientation is isotropic, the reduced spectral-density function can be written as

$$J(\omega) = \frac{2}{5}\left(\frac{S^2\tau_M}{1 + \omega^2\tau_M^2} + \frac{(1 - S^2)\tau}{1 + \omega^2\tau^2}\right) \quad (4)$$

where $\tau^{-1} = \tau_M^{-1} + \tau_e^{-1}$. τ_M is the correlation time for the global motion, common to the whole molecule, τ_e is the correlation time for the fast local motion, specific for every individual axis in the molecule, and S is a generalized order parameter. S reflects the spatial restriction of the local motion. If the first term in eq 4 is much larger than the second, eq 4 can be truncated to obtain

$$J(\omega) = \frac{2}{5}\left(\frac{S^2\tau_M}{1 + \omega^2\tau_M^2}\right) \quad (5)$$

which is identical with the expression for isotropic small-step diffusion of a rigid molecule[32] with an amplitude scaling factor S^2.[14] If the product $\omega^2\tau_M^2 \ll 1$ at all the relevant frequencies (the extreme-narrowing conditions), the relaxation parameters do not depend on the magnetic field and the determination of S^2 and τ_M independently of each other is not possible.

More sophisticated models, allowing for the anisotropy of the overall reorientation, have been proposed.[33−35] In our earlier work,[23,26] we have seen indications of anisotropy effects such as different global correlation times obtained for different fragments of a molecule, an effect that has been investigated by Schurr and co-workers[35] using a different data-analysis protocol. The possible motional anisotropy can be estimated from the elements of the moment of inertia tensor for the two molecules. In both cases, the tensors turn out to be only moderately anisotropic (the ratio of principal components for the global energy-minimum conformer is 1:0.67:0.45 for **1** and 1:0.64:0.51 for **2**). This anisotropy happens to be rather similar

TABLE 1: Averaged[a] Relaxation Data for the Trisaccharides[b] 1 and 2 at Three Temperatures and Four Magnetic Fields

T (K)	B_0 (T)		1				2		
			g	**g²**	**g³**	**gC6**	**m**	**g²**	**g³**
283	6.34	T_1	133[c]	136	134	73	119	123	126
		$1+\eta$	1.33	1.57	1.53	1.43	1.33	1.46	1.53
283	9.39	T_1	194	204	204	113	197	209	212
		T_2	102	122	115	62	93	121	110
		$1+\eta$	1.26	1.37	1.33	1.34	1.21	1.36	1.36
283	11.74	T_1	274	278	277	157	245	258	252
		$1+\eta$	1.19	1.26	1.25	1.25	1.16	1.27	1.29
303	6.34	T_1	151	172	169	86	145	184	193
		$1+\eta$	1.82	1.98	1.96	1.92	1.83	2.03	2.05
303	9.39	T_1	203	231	228	124	195	231	236
		T_2	154	182	179	92	142	187	183
		$1+\eta$	1.53	1.69	1.66	1.64	1.62	1.82	1.89
303	11.74	T_1	242	271	266	149	234	273	269
		$1+\eta$	1.40	1.55	1.55	1.47	1.40	1.57	1.64
303	14.09	T_1	282	319	307	172	278	315	320
		$1+\eta$	1.37	1.54	1.52	1.43	1.34	1.50	1.55
323	6.34	T_1	196	252	246	124	188	251	262
		$1+\eta$	2.65	2.79	2.72	2.73	2.46	2.57	2.56
323	9.39	T_1	246	288	294	153	230	286	302
		T_2	198	257	241	125	187	259	252
		$1+\eta$	2.16	2.25	2.27	2.16	2.18	2.35	2.34
323	11.74	T_1	265	319	318	169	267	336	347
		$1+\eta$	1.82	2.02	2.03	1.91	1.80	2.01	2.04
323	14.09	T_1	318	378	370	200			
		$1+\eta$	1.77	1.95	1.94	1.87			

[a] Relaxation data are averaged from measurements of well-resolved signals in each sugar residue employing "dynamical equivalence" for individual sugar residues. [b] Glucose and mannose residues are denoted by **g** and **m**, respectively, with superscripts indicating the linkage positions (cf. Figure 1). The exocyclic hydroxymethyl group of **g** in **1** is denoted **gC6**. [c] T_1 and T_2 values are given in ms.

to that reported in a ^{15}N relaxation study of ubiquitin by Tjandra et al.[34] where the principal components were 1:0.90:0.64. In that work, the anisotropy of the moment of inertia tensor translates into a significally smaller anisotropy of the axially symmetric rotational diffusion tensor ($D_\parallel/D_\perp = 1.17$). Given the fact that both proteins[36] and oligosaccharides[37,38] are strongly hydrated, it is reasonable that also in the present case the anisotropy of the diffusion tensor is lower than the anisotropy of the moment of inertia tensor. Following Schurr et al.,[35] the errors caused by use of the simple, isotropic Lipari−Szabo model should in such a case be rather small. We choose therefore to use the simple isotropic model.

Experimental Section

The synthesis of trisaccharides **1** and **2** has been described.[39] Prior to relaxation measurements, the trisaccharides were treated with CHELEX 100 in order to remove any paramagnetic ions present. A solvent mixture of 70 mol % ^2H_2O and 30 mol % DMSO-d_6 was used in order to create conditions outside of the extreme-narrowing regime by slowing the molecular reorientation (through the increased viscosity). Solutions of the trisaccharides, 0.1 M, were transferred to 5-mm NMR tubes, which were sealed under vacuum after degassing by the freeze−pump−thaw procedure. The ^{13}C-NMR spectra of compounds **1** and **2** were assigned as previously reported.[39] For **1**, the resonance lines of glucose residues **g** C1−C6, **g²** C1−C2, and **g³** C1−C2 were well-resolved and accordingly used for measurements. For **2**, mannose residue **m** C1, C2, and C4 and glucose residues **g²** C1 and C4 and **g³** C1, C2, and C4 were used at all temperatures and magnetic fields, and when the resolution was sufficient, more carbon peaks were used.

Carbon-13 T_1 and NOE experiments were performed at four magnetic fields using JEOL GSX 270 (6.3 T), JEOL Alpha 400 (9.4 T), Varian Unity 500 (11.7 T), and Varian Unity *plus* 600 (14.1 T) spectrometers. Carbon-13 T_2 measurements were performed with a JEOL Alpha 400 spectrometer (9.4 T). Standard pulsed proton broad-band decoupling techniques were used, with the decoupling power attenuated in order to avoid sample heating. A deuterium lock was used for the field/frequency stabilization. The spectral window covered 60−80 ppm, and the number of data points was 8K or 16K. The number of transients for a given delay time τ in the two to five independent measurements of a relaxation parameter were on the order of 1000. Standard variable-temperature equipment provided by the manufacturers was used with all instruments. The temperature calibration was carried out using the proton-shift thermometer[40] and/or an electronic thermometer calibrated in ice and boiling water. Experiments were performed at three temperatures: 283 ± 2, 303 ± 2, and 323 ± 2 K.

An average over the independent measurements for each experimental parameter, i.e., T_1, T_2, and $1+\eta$, was calculated for each of the resolved signals. In the case that a measured value deviated more than ±10% from the average, it was discarded and a new average was subsequently calculated. If needed, the procedure was repeated until the above criterion was fulfilled. At this point the "dynamic equivalence"[24] of the sugar residues was applied to calculate an average experimental parameter for each sugar residue at a certain temperature and field, i.e., to give the entries in Table 1. To estimate the variation in the experimental data, the standard deviation was calculated for each resonance. An average standard deviation was then calculated from the standard deviations for each experimental parameter over all temperatures and fields and was found to be 4% for T_1, T_2, and $1+\eta$. All the relaxation measurements were performed as direct-detection experiments. It is our experience that, for molecules of this size, the more sophisticated inverse-detection techniques offer little advantage.[41]

For T_1 measurements, the fast inversion−recovery method[42] was used in combination with a three-parameter nonlinear fitting

of line intensities, using standard software provided with the spectrometers. The number of τ delays was around 10.

The NOE measurements were performed using the dynamic NOE technique with reduced decoupling power during the NOE buildup time.[43] The recovery delay between transients was set to $>10T_1$. Commonly, five or six different τ delays were employed, but at 283 K at 6.3 and 11.8 T and at 303 and 323 K at 14.1 T, one short (10 ms) and one long (about $5T_1$) irradiation period were used. The NOEs $(1 + \eta)$ were calculated by two-parameter nonlinear fits of the line intensities or by taking the ratio of the long irradiation period to the short irradiation period.

Carbon-13 T_2 measurements were performed according to a modified Carr−Purcell−Meiboom−Gill experiment,[26,31] with the CPMG delay set to 250 μs, a proton π-pulse length of 13.8 μs and a carbon π-pulse length of 16 μs. The recovery delay was $>4T_1$. Spectra with 10 τ values were recorded for each experiment.

The Lipari−Szabo model parameters S^2, τ_M, and τ_e were least-squares-fitted to the relaxation parameters of the residue-averaged data for **1** and **2** and one of the methylene carbons in **1** (Table 1) using the program GENLSS[44] running on a Silicon Graphics Inc. workstation. Sums of squares of relative (rather than absolute) errors were minimized, which allowed treatment of the measured parameters (T_1^{-1}, T_2^{-1}, $(1 + \eta)$) in a balanced way.

Results and Discussion

The motional properties of trisaccharides **1** and **2** have been investigated in a solvent mixture of ^2H_2O:DMSO-d_6 (7:3). The higher viscosity of this solvent mixture, compared with that of water, brings the trisaccharides with a molecular mass of ∼500 Da outside the extreme-narrowing regime, where measurements of spin−lattice and spin−spin relaxation rates and NOE give valuable information about the internal motions.[32] In addition, this mixture is characterized by a large decrease of the freezing point, which allows NMR measurements at lower temperatures (cryosolvent). The solvent mixture contains 70% water, and a comparative study, in which long-range heteronuclear coupling constants have been measured in both water and the cryosolvent mixture, shows small changes, i.e., within the experimental error of the technique, in the $^3J_{C,H}$ values for the oligosaccharides in the two solvents.[45] We interpret this observation as showing that, to a good approximation, the solvating properties of the mixed solvent are similar to those of water and that the choice of the cryosolvent is justified in order to facilitate the magnetic-field-dependent studies. Furthermore, according to McCain and Markley[46,47] neither the overall molecular dimensions nor the pattern of internal motions varies for sucrose at concentrations of 0.1−1.0 M. Additionally, τ_c for sucrose at 0.1 M aqueous solution is similar to that at the infinite dilution limit.

Trisaccharides **1** and **2** both consist of two terminal β-glucosyl residues that are vicinally substituted at positions 2 (residue $\mathbf{g^2}$) and 3 (residue $\mathbf{g^3}$) of a methyl glucoside (**g** in compound **1**) or a methyl mannoside (**m** in compound **2**), as shown in Figure 1. Trisaccharide **1** has the two β-glucosyl residues oriented equatorially in space with respect to the average plane of the methyl glucoside ring carbons. Trisaccharide **2**, however, has one equatorially and one axially oriented β-glucosyl residue, resulting in a different geometry.

The compounds have been studied earlier by Monte Carlo simulations and analysis of chemical-shift differences,[39] from which it was indicated that no large differences in three-dimensional structure had occurred for the trisaccharides in comparison with their constituent disaccharides. A difference in conformational flexibility of the glycosidic linkages between the trisaccharides as well as between the trisaccharide **2** and its constituent disaccharides was suggested from the MC calculations. Trisaccharide **1** showed similar flexibility at the (1 → 2) and (1 → 3) glycosidic linkages, while trisaccharide **2** had larger flexibility at the equatorial (1 → 3) glycosidic linkage compared with that at the axial (1 → 2) linkage.

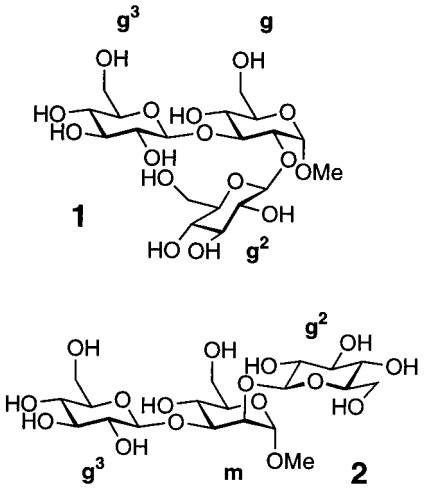

Figure 1. Schematic representation of trisaccharides **1** and **2**. The methyl glucoside of compound **1** and the methyl mannoside of compound **2** are denoted **g** and **m**, respectively. The terminal β-glucosyl residues are named $\mathbf{g^2}$ and $\mathbf{g^3}$, from the position they substitute.

Longitudinal (T_1) and transverse (T_2) relaxation times complemented with ^1H, ^{13}C NOE were measured for **1** and **2** at four magnetic-field strengths and three temperatures. The relaxation data for individual carbons in each sugar residue of **1** and **2** were found to be similar, generally within ±5% from the average of the residue, and therefore, the carbons were treated as dynamically equivalent.[24] The data were averaged for each individual sugar residue at each temperature and magnetic field, as shown in Table 1. The averaged relaxation data were used to calculate the Lipari−Szabo parameters τ_M, S^2, and τ_e for the three sugar residues of **1** and **2** at 283, 303, and 323 K. Three different fits were performed: (i) least-squares fitting of the overall correlation time τ_M and the squared order parameter S^2 using a very short (10^{-15} s) fixed value of the internal correlation time τ_e, corresponding to the truncated form of the Lipari−Szabo model (eq (5); (ii) simultaneous least-squares fitting of τ_M, S^2, and τ_e; (iii) least-squares fitting of S^2 and τ_e with τ_M fixed to the value obtained for the methyl glycoside residue in the first fit. The results are given in Tables 2 and 3 and the quality of the fits is illustrated in Figures 2 and 3.

The relaxation data clearly show differences in the motional behavior of the different sugar residues. At 283 K, the T_1 values of the different residues are fairly similar while the NOE and T_2 values for the terminal β-glucosyl residues $\mathbf{g^2}$ and $\mathbf{g^3}$ are larger compared with that of the methyl glucoside/mannoside residues **g** and **m** in trisaccharides **1** and **2**. The T_1/T_2 ratio is large and strongly field-dependent at 283 K. In this slow-rotation regime, accurate measurements of T_2 seem to be necessary for a successful analysis, since the NOE values are small and less field-dependent. At 303 and 323 K the relaxation data show similar but larger differences in T_1, T_2, and NOE $(1 + \eta)$ between the terminal and central residues, but the field dependence of the relaxation times is not as strong. The NOE data at 323 K and lower magnetic-field strengths are in the

TABLE 2: Results from Two-Parameter Least-Square Fits of Ring Carbons in Individual Sugar Residues in Trisaccharides 1 and 2

compound	residue	T (K)	τ_M (ns)	S^2	Δy^a
1	**g**	283	1.90 ± 0.06	0.87 ± 0.01	2.7
	g²	283	1.47 ± 0.10	0.82 ± 0.02	4.8
	g³	283	1.61 ± 0.09	0.83 ± 0.02	4.4
1	**g**	303	0.86 ± 0.02	0.86 ± 0.01	1.9
	g²	303	0.68 ± 0.02	0.79 ± 0.01	3.2
	g³	303	0.69 ± 0.02	0.80 ± 0.01	3.1
1	**g**	323	0.42 ± 0.02	0.88 ± 0.03	5.1
	g²	323	0.34 ± 0.02	0.78 ± 0.02	4.3
	g³	323	0.34 ± 0.02	0.79 ± 0.02	4.4
2	**m**	283	2.02 ± 0.07	0.93 ± 0.01	2.9
	g²	283	1.50 ± 0.10	0.85 ± 0.02	4.9
	g³	283	1.58 ± 0.14	0.86 ± 0.03	6.4
2	**m**	303	0.86 ± 0.04	0.89 ± 0.02	3.3
	g²	303	0.63 ± 0.02	0.79 ± 0.01	3.2
	g³	303	0.59 ± 0.04	0.80 ± 0.02	5.5
2	**m**	323	0.44 ± 0.03	0.90 ± 0.03	5.1
	g²	323	0.35 ± 0.02	0.76 ± 0.02	3.4
	g³	323	0.35 ± 0.03	0.74 ± 0.03	5.1

[a] Standard deviation of the dependent variable (%).

vicinity of the extreme-narrowing limit ($\omega^2\tau_M^2 \ll 1$) and may not be very sensitive to motional differences.

From the two-parameter fits of τ_M and S^2 (Table 2) for each residue of compounds **1** and **2**, we note that the overall correlation time τ_M decreases with increasing temperature for all sugar residues but that it is somewhat shorter for the terminal residues **g²** and **g³** than for the **g** and **m** residues at all studied temperatures. The τ_M of the Lipari−Szabo model should in principle be common for the whole molecule, and the motions obtained here indicate deviations from the model, possibly due to anisotropic motion.[33,34] The squared order parameter S^2 is found to be constant with temperature in the range 283−323 K for the branch-point residues **g** and **m** of compounds **1** and **2**. The truncated form of the Lipari−Szabo equation, eq 5, can be used when the order parameter squared is high and the second term in the Lipari−Szabo equation becomes negligible (a fairly rigid molecule). In such a case, the short local correlation time cannot be obtained with confidence. This seems to be the case (vide infra) for the branch-point residues **g** and **m** for which S^2 values of 0.86−0.93 are found at the studied temperatures. For residues **g²** and **g³** of **1** and **2**, the order parameters are slightly temperature-dependent with the highest values ($S^2 = 0.82-0.86$) at 283 K and the lowest values ($S^2 = 0.74-0.79$) at 323 K. This trend is the same as in earlier observations, for example, for melezitose.[25] The S^2 values for the terminal residues at the two higher temperatures may be low enough to allow an estimation of τ_e. The temperature dependence of S^2 for the terminal β-glucosyl residues seems to be larger for trisaccharide **2** ($S^2 = 0.74-0.86$) than for trisaccharide **1** ($S^2 = 0.78-0.83$), suggesting somewhat different motional properties of the terminal groups in the two trisaccharides.

In the second step of the analysis, a simultaneous three-parameter fit of τ_M, S^2, and τ_e using eq 4 was performed (Table 3) for the data at 283 and 303 K. For residues **g** and **m** this fit gave results similar to results from the two-parameter fit of τ_M and S^2, with high values of the squared order parameters (S^2 0.84−0.95) and similar overall correlation times. At 283 K negative (unphysical) values of τ_e were obtained, and at 303 K small τ_e values (∼20 ps) with large errors ($> \tau_e$) were found. This is in agreement with our earlier experience for sugar residues with limited internal mobility.[24−26] Similar results with large errors in τ_e, but with $S^2 \approx 0.8$, were also obtained for the terminal β-glucosyl residues **g²** and **g³** of both trisaccharides at 283 K.

For residues **g²** and **g³** of **1** at 303 K, the three-parameter fit showed a significant improvement compared to the two-parameter case: the standard deviation of the measured relaxation rates (dependent variable), compared with the back-calculated least-squares-fitted rates, dropped to about half. The least-squares-fitted motional parameters changed significantly. The τ_M values for the **g²** and **g³** residues of **1** at 303 K in Table 3 are longer than in Table 2, i.e., closer to the values for the methyl glucoside **g**, and the order parameters squared are around 0.7. In agreement with this indication of more extended local mobility, it was possible also to quantify the local correlation time τ_e to ∼60 ± 10 ps for both the terminal residues of **1** at 303 K. The data in Table 3 clearly show that the dynamic properties of the two terminal units are very similar and that the motions of the methyl glucoside **g** and the terminal residues **g²** and **g³** are different.

The trend for the terminal residues in **2** at 303 K is similar but less distinct. Also, in this case the τ_M values for the terminal β-glucosyl residues are longer in the three-parameter fit (Table 3) than in the two-parameter fit of τ_M and S^2 (Table 2) and the order parameters squared are lower, but the uncertainties in Table 3 are rather large for both **g²** and **g³** in **2**. The **g³** residue seems to be somewhat more flexible (slightly lower S^2) compared with the **g²** residue (cf. MC simulations); τ_e was found to be significantly longer for the terminal residue **g³**, but the τ_e values are on the border of being insignificant. It is thus rather difficult to draw conclusions on the possible differences in the dynamic behavior of residues **g²** and **g³** in **2**.

We also attempted to fit the 323 K data for **1** and **2** using the same three-parameter procedure but were not successful. This

TABLE 3: Results from Three-Parameter Least-Square Fits of Ring Carbons and One Hydroxymethyl Carbon in Individual Sugar Residues in Trisaccharides 1 and 2

compound	residue	T (K)	τ_M (ns)	S^2	τ_e (ps)	Δy^a
1	**g**	283	1.89 ± 0.07	0.87 ± 0.02	$(-8.7 \pm 24)^b$	2.9
	g²	283	1.56 ± 0.12	0.79 ± 0.03	31 ± 28	4.8
	g³	283	1.68 ± 0.11	0.81 ± 0.02	30 ± 25	4.3
	gC6	283	1.80 ± 0.07	0.73 ± 0.01	20 ± 11	2.9
1	**g**	303	0.89 ± 0.03	0.84 ± 0.02	18 ± 19	1.9
	g²	303	0.80 ± 0.03	0.70 ± 0.02	57 ± 10	1.6
	g³	303	0.81 ± 0.03	0.72 ± 0.02	58 ± 9	1.4
	gC6	303	0.84 ± 0.06	0.69 ± 0.03	21 ± 16	3.5
2	**m**	283	1.97 ± 0.07	0.95 ± 0.02	$(-86 \pm 89)^b$	2.5
	g²	283	1.56 ± 0.13	0.83 ± 0.03	29 ± 37	5.1
	g³	283	1.72 ± 0.15	0.82 ± 0.03	70 ± 42	5.7
2	**m**	303	0.88 ± 0.07	0.88 ± 0.04	17 ± 48	3.6
	g²	303	0.68 ± 0.05	0.75 ± 0.04	33 ± 25	3.2
	g³	303	0.71 ± 0.10	0.69 ± 0.07	67 ± 36	5.2

[a] Standard deviation of the dependent variable (%). [b] Unphysical result, $\tau_e < 0$.

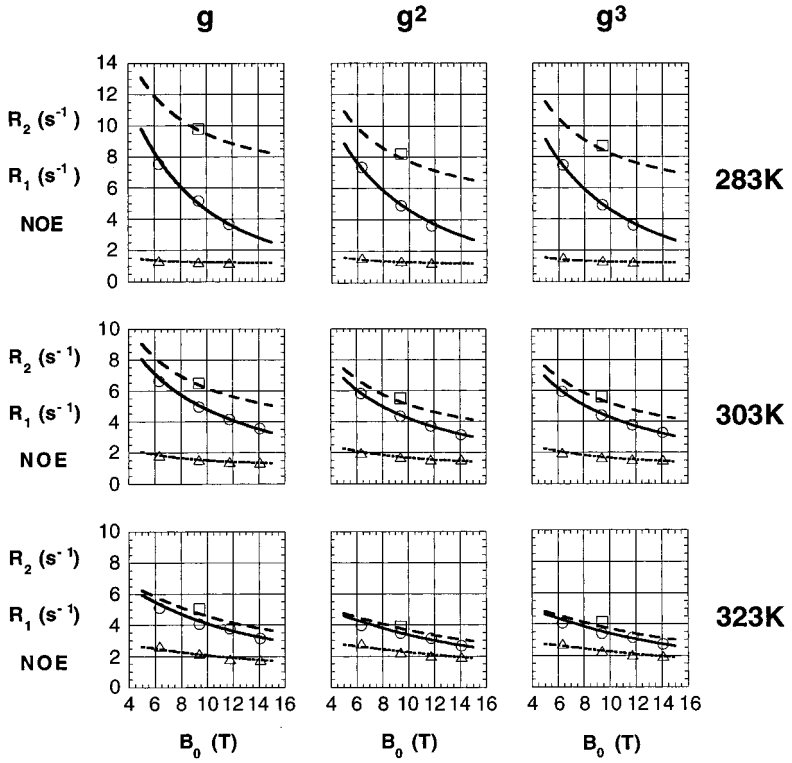

Figure 2. Plots of calculated T_1^{-1} (solid lines), T_2^{-1} (dashed), and $1 + \eta$ (dotted) values for the ring carbons of trisaccharide **1**. The plots of each residue **g**, $\mathbf{g}^2$, and $\mathbf{g}^3$ are shown vertically at the three different temperatures 283 K (upper row), 303 K (middle), and 323 K (lower). Shown also are the experimental values of T_1^{-1} (○), T_2^{-1} (□), and $1 + \eta$ (△). The lines are calculated from data in Table 2.

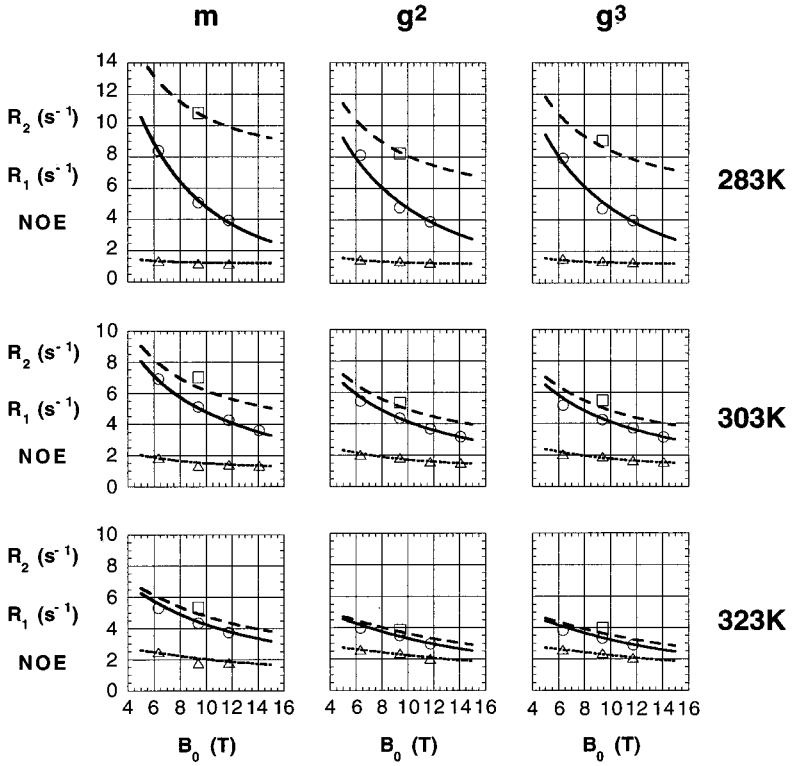

Figure 3. Plots of calculated T_1^{-1} (solid lines), T_2^{-1} (dashed), and $1 + \eta$ (dotted) values for the ring carbons of trisaccharide **2**. The plots of each residue **m**, $\mathbf{g}^2$, and $\mathbf{g}^3$ are shown vertically at the three different temperatures 283 K (upper row), 303 K (middle), and 323 K (lower). Shown are also the experimental values of T_1^{-1} (○), T_2^{-1} (□), and $1 + \eta$ (△). The lines are calculated from data in Table 2.

failure is probably due to the fact that the data at 323 K show rather less field- dependence (cf. Figures 2 and 3), i.e., are actually close to the extreme-narrowing conditions. The overall and internal motions may also come closer to each other as τ_M decreases, and thereby, one important criterion of the Lipari−Szabo method, namely, $\tau_e \ll \tau_M$, may not be fulfilled.

Because of spectral overlap, only one of the six exocyclic hydroxymethyl carbons in **1** and **2** could be used for relaxation

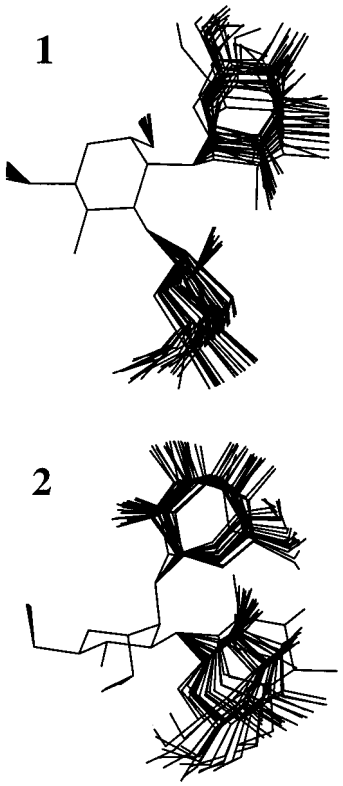

Figure 4. Plot of 20 random structures of trisaccharides **1** and **2** from Monte Carlo simulations (10^6 steps at 300 K), showing the conformational space around the glycosidic linkages. The overlay plots are based on the branch-point residues.

measurements. The relaxation data for the exocyclic carbon C6 of the **g** residue in trisaccharide **1** at 283 and 303 K were fitted using the simultaneous three-parameter fit of τ_M, S^2, and τ_e. The results are presented in Table 3. The overall correlation times of C6 and C1−C5 of the **g** residue were of the same magnitude at both temperatures, with deviations within the error limits. The squared order parameter S^2 of C6 in **g** was ∼0.7 at the two temperatures, a reduction compared with that in the **g** residue, for which $S^2 \approx 0.85$ was found. The internal correlation time τ_e was found to be ∼20 ps at both temperatures, within large error limits (±11−16 ps). These results show an increased mobility of the hydroxymethyl group compared with the ring carbons of the sugar residue they are part of and agree with results of previous studies.[23−26,48]

To get a better interpretation of the data at 323 K, we performed two-parameter fits of S^2 and τ_e for the terminal residues $\mathbf{g}^2$ and $\mathbf{g}^3$ in **1** and **2** at all three temperatures, with the overall correlation time fixed to the value obtained from the two-parameter fit in Table 2 for the central sugar residues **g** or **m** at each temperature. The results for $\mathbf{g}^2$ and $\mathbf{g}^3$ in **1** at 283 and 303 K (not shown) are similar to the data in Table 3 but with somewhat larger standard deviation of the dependent variable and with τ_e values of ∼60 ps at 283 K. At 323 K, the squared order parameters of the terminal β-glucosyl residues of **1** were close to 0.6 and the local correlation times came out as 80 ± 30 ps. The results for trisaccharide **2** at 283 and 303 K are less conclusive. The τ_e values of the terminal residues were slightly below 100 ps and larger compared with the values obtained from the three-parameter fits. At 323 K the two-parameter fits gave rather low order parameters ($S^2 = 0.53 \pm 0.04$ and 0.55 ± 0.06 for $\mathbf{g}^2$ and $\mathbf{g}^3$, respectively) and τ_e values of about 90 ± 30 ps. Thus, the results indicate, as expected, increased flexibility for the terminal residues at higher temperatures.

The two-parameter fit of S^2 and τ_e was also performed for the exocyclic carbon C6 in **g** at all three temperatures, using the τ_M value of the methyl glucoside **g** as the fixed overall correlation time. At 283 and 303 K both S^2 and τ_e were found to be similar to the values obtained with the three-parameter fit. At 323 K the fit resulted in a S^2 value of 0.66 ± 0.03 and an internal correlation time τ_e of 27 ± 21 ps.

The results obtained in this study are not inconsistent with the results from the MC simulations.[39] Similar energy landscapes, indicating comparable motional properties, were found for the terminal residues of trisaccharides **1** and **2** in both studies; namely, no large difference in flexibility between the terminal residues was found for **1**, whereas in **2** the (1 → 2) linkage was found to be less flexible and the (1 → 3) linkage more flexible compared with the corresponding linkages in trisaccharide **1**. Since high S^2 values were found for the branch-point residues in this study we have chosen to make use of the MC calculations by overlay of these residues to make a pictorial model of the conformational flexibility of the (1 → 2)- and (1 → 3) linkages in the two trisaccharides as shown in Figure 4.

Concluding Remarks

Relaxation data measured at four magnetic field strengths have been fitted at 283, 303, and 323 K to obtain motional parameters according to the Lipari−Szabo model-free approach. All fits at 303 K were straightforward and resulted in τ_M, S^2, and τ_e values within reasonable error limits. At 283 and 323 K the fitting procedures often failed or resulted in motional parameters with large errors. The reason for these observations must be related to the field dependence of the measured relaxation parameters, to signal-to-noise ratios in the performed experiments, and to the sensitivity of the relaxation parameters to changes in τ_M. NOE $(1 + \eta)$ values of ∼2 in the middle of the theoretical range should be most sensitive to variations of the magnetic field and accordingly result in good fits. Measurements close to the extreme-narrowing regime, e.g., at higher temperatures, are not as field-dependent and are less sensitive to internal motions. When the NOE values are near the theoretical minimum, they become effectively independent of motional parameters and the magnetic field. In this range, carbon-13 T_2 measurements show a larger field dependence and give more motional information. The temperature, the viscosity, and to a lesser extent the magnetic field strength(s) should be chosen in such a way to find the range where the relaxation parameters are most sensitive to variations of the dynamic parameters and of the field.

The ^{13}C relaxation data have been interpreted for the trans- and cis-disubstituted trisaccharides **1** and **2**, respectively, using the "model-free" approach of Lipari and Szabo. The carbon atoms in each sugar ring were treated as dynamically equivalent. The disubstituted *O*-methyl glycoside showed for both trisaccharides the highest S^2 value of ∼0.9. The terminal glucosyl groups had lower S^2 values of ∼0.8 when a two-parameter fit of τ_M and S^2 was employed. This fit also showed a slight temperature dependence of the S^2 values for the terminal groups, larger for **2** than for **1**, with higher order parameters at lower temperatures. Three-parameter fits identified internal correlation times τ_e for the terminal glucosyl groups of trisaccharide **1** to be about 60 ps. No significant difference in flexibility was observed between these groups, in accordance with previous Monte Carlo simulations. For trisaccharide **2**, similar results for S^2 and τ_e were obtained but with some differences between the terminal residues and larger errors. For the hydroxymethyl group of the *O*-methyl glucoside residue in **1** a lower order

parameter squared, compared with that of the ring, of ~0.7 with $\tau_e \approx 20$ ps was observed, as in previous studies. The relaxation data in the present study facilitate the interpretation and differentiation of a core sugar with restricted mobility substituted by more flexible terminal sugar residues.

Acknowledgment. This work was supported by grants from the Swedish Natural Science Research Council. The Swedish NMR Centre is thanked for providing access to the U500 NMR spectrometer.

References and Notes

(1) Doddrell, D.; Glushko, V.; Allerhand, A. *J. Chem. Phys.* **1972**, *56*, 3683.
(2) Peng, J. W.; Wagner, G. *J. Magn. Reson.* **1992**, *98*, 308.
(3) Lipari, G.; Szabo, A. *J. Am. Chem. Soc.* **1982**, *104*, 4546.
(4) Arvidsson, K.; Jarvet, J.; Allard, P.; Ehrenberg, A. *J. Biomol. NMR* **1994**, *4*, 653.
(5) Smith, P. E.; van Schaik, R. C.; Szyperski, T.; Wüthrich, K.; van Gunsteren, W. F. *J. Mol. Biol.* **1995**, *246*, 356.
(6) Cavanagh, J.; Fairbrother, W. J.; Palmer, A. G., III; Skelton, N. J. *Protein NMR spectroscopy: principles and practice*; Academic Press: San Diego, 1996.
(7) Borer, P. N.; LaPlante, S. R.; Kumar, A.; Zanatta, N.; Martin, A.; Hakkinen, A.; Levy, G. C. *Biochemistry* **1994**, *33*, 2441.
(8) Bouchemal-Chibani, N.; du Penhoat, C. H.; Abdelkafi, M.; Ghomi, M.; Turpin, P. Y. *Biopolymers* **1996**, *39*, 549.
(9) Scheiffele, P.; Peränen, J.; Simons, K. *Nature* **1995**, *378*, 96.
(10) Crocker, P. R.; Feizi, T. *Curr. Opin. Struct. Biol.* **1996**, *6*, 679.
(11) Woods, R. J. *Curr. Opin. Struct. Biol.* **1995**, *5*, 591.
(12) Peters, T.; Meyer, B.; Stuike-Prill, R.; Somorjai, R.; Brisson, J.-R. *Carbohydr. Res.* **1993**, *238*, 49.
(13) Widmalm, G.; Venable, M. *Biopolymers* **1994**, *34*, 1079.
(14) Levy, R. M.; Karplus, M. *J. Am. Chem. Soc.* **1981**, *103*, 994.
(15) Levy, R. M.; Karplus, M. *Adv. Chem. Ser.* **1983**, *204*, 445.
(16) Koning, T. M. G.; Boelens, R.; van der Marel, G. A.; van Boom, J. H.; Kaptein, R. *Biochemistry* **1991**, *30*, 3787.
(17) Norberg, J.; Nilsson, L. *J. Biomol. NMR* **1996**, *7*, 305.
(18) van Halbeek, H. *Curr. Opin. Struct. Biol.* **1994**, *4*, 697.
(19) Peters, T.; Pinto, B. M. *Curr. Opin. Struct. Biol.* **1996**, *6*, 710.
(20) Nishida, T.; Widmalm, G.; Sándor, P. *Magn. Reson. Chem.* **1995**, *33*, 596.
(21) Nishida, T.; Widmalm, G.; Sándor, P. *Magn. Reson. Chem.* **1996**, *34*, 377.
(22) Dais, P. *Adv. Carbohydr. Chem. Biochem.* **1995**, *51*, 63.
(23) Bagley, S.; Kovacs, H.; Kowalewski, J.; Widmalm, G. *Magn. Reson. Chem.* **1992**, *30*, 733.
(24) Kowalewski, J.; Widmalm, G. *J. Phys. Chem.* **1994**, *98*, 28.
(25) Mäler, L.; Lang, J.; Widmalm, G.; Kowalewski, J. *Magn. Reson. Chem.* **1995**, *33*, 541.
(26) Mäler, L.; Widmalm, G.; Kowalewski, J. *J. Biomol. NMR* **1996**, *7*, 1.
(27) Mäler, L.; Widmalm, G.; Kowalewski, J. *J. Phys. Chem.* **1996**, *100*, 17103.
(28) Werbelow, L. G.; Grant, D. M. *Adv. Magn. Reson.* **1977**, *9*, 189.
(29) Canet, D. *Prog. Nucl. Magn. Reson. Spectrosc.* **1989**, *21*, 237.
(30) Palmer, A. G., III; Skelton, N. J.; Chazin, W. J.; Wright, P. E.; Rance, M. *Mol. Phys.* **1992**, *75*, 699.
(31) Kay, L. E.; Nicholson, L. K.; Delaglio, F.; Bax, A.; Torchia, D. A. *J. Magn. Reson.* **1992**, *97*, 359.
(32) Kovacs, H.; Bagley, S.; Kowalewski, J. *J. Magn. Reson.* **1989**, *85*, 530.
(33) Barbato, G.; Ikura, M.; Kay, L. E.; Pastor, R. W.; Bax, A. *Biochemistry* **1992**, *31*, 5269.
(34) Tjandra, N.; Feller, S. E.; Pastor, R. W.; Bax, A. *J. Am. Chem. Soc.* **1995**, *117*, 12562.
(35) Schurr, J. M.; Babcock, H. P.; Fujimoto, B. S. *J. Magn. Reson.* **1994**, *B105*, 211.
(36) Venable, R. M.; Pastor, R. W. *Biopolymers* **1988**, *27*, 1001.
(37) Einstein, A. *Ann. Phys.* **1906**, *19*, 289; **1911**, *34*, 591.
(38) Engelsen, S. B.; Pérez, S. *Carbohydr. Res.* **1996**, *292*, 21.
(39) Jansson, P.-E.; Kjellberg, A.; Rundlöf, T.; Widmalm, G. *J. Chem. Soc., Perkin Trans. 2* **1996**, 33.
(40) Ammann, C.; Meier, P.; Merbach, A. E. *J. Magn. Reson.* **1982**, *46*, 319.
(41) Kowalewski, J.; Mäler, L. Measurements of relaxation rates for low natural abundance I=1/2 nuclei. In *Methods for structure elucidation by high-resolution NMR*; Batta, G., Kövér, K. E., Szántay, C., Eds.; Elsevier: London, 1997.
(42) Canet, D.; Levy, G. C.; Peat, I. R. *J. Magn. Reson.* **1975**, *18*, 199.
(43) Kowalewski, J.; Ericsson, A.; Vestin, R. *J. Magn. Reson.* **1978**, *31*, 165.
(44) DeTar, D. F. *Computer Programs for Chemistry*; Academic Press: New York, 1972; Vol. 4.
(45) Rundlöf, T.; Kjellberg, A.; Damberg, C.; Nishida, T.; Widmalm, G. Manuscript in preparation.
(46) McCain, D. C.; Markley, J. M. *J. Am. Chem. Soc.* **1986**, *108*, 4259.
(47) McCain, D. C.; Markley, J. M. *Carbohydr. Res.* **1986**, *152*, 73.
(48) McCain, D. C.; Markley, J. L. *J. Magn. Reson.* **1987**, *73*, 244.